72nd IIW Annual Assembly and International Conference
7–12 July 2019 Conference Proceedings

Effect of the spot welding simulation strategy on analysis of performance in automotive parts

Mahyar Asadi[1,a], Majid Tanbakuei Kashani[1,b], Chris Timbrell[2,c], Ramesh Chandwani[2,d], Mathew Smith[1,e]

[1]Advanced Welding Engineering Services, Applus Canada - SKC Engineering, North Vancouver, Canada
[2]Research & Development, Zentech International Limited, London, United Kingdom

[a]mahyar.asadi@applusrtd.com, [b]majid.kashani@applusrtd.com, [c]chris@zentech.co.uk, [d]ramesh@zentech.co.uk,
[e]mathew.smith@applusrtd.com

Abstract

Spot weld plays a critical role in the integrity of automotive and fatigue durability of the body over the course of service. Numerical analysis is a common tool to model the behaviour of spot welds in automotive under both service and crash loading. However, the modeling strategy can significantly change the result of analysis and therefore the final engineering decision. Authors observed that modelers typically define the spot welds as a mechanical tie between two plates and ignore the local effect from welding process that changes the material properties in weld nugget and the surrounding Heat Affected Zone (HAZ). However, spot welding leads to property evolution to higher strength and toughness and lower ductility in the weld nugget than parents metal's property. This evolution is opposite in HAZ with lesser strength and toughness and higher ductility than parents metal's property. This local effect at the weld region changes the stress-strain behaviour of the structure and it becomes more significant when dealing with fatigue life prediction because fatigue is a local phenomenon and the analysis of fatigue uses the local stress and strain for life calculation. Therefore the simulation of welding process needs to be part of the analysis for making a realistic decision. On the other hand, welding modeling could take longer CPU time for a large number of welding involved in the automotive body such that it is not feasible to model every individual welding process. Here, authors compared two modeling scenarios where one defines the weld as mechanical tie vs. the other one that includes the modeling of welding process and evolution of material properties in the weld metal and HAZ. The main criteria for the comparison are the fatigue durability and crack evolution in the weld nuggets and the structure. We also proposed a methodology to avoid the repetitive weld modeling for every weld nuggets and using the result of characteristic welds to cover all welding locations in the structure.

Keywords
simulation, HAZ, welding, automotive, crash

1. Introduction

Spot resistance welding is the critical joining process in the automotive body-in-white assembly with a car comprising thousands of spot welds that connect parts with a wide-ranging variety of configuration involving different thickness, materials, numbers of sheet metals, size of welds, and so on. The quality of spot welds, and subsequently, the performance of the joint, depends on many parameters, for example, Dipak and Ganesh [1] summarized many parameters that can affect the spot weld strength. The fusion nature of spot resistance welding complicates the evaluation of performance and failure for spot welded joints. Poranvari and Marashi [2] correlated the fusion understanding of the spot welding process to the structural property of the automotive component. They identified three microstructural zones namely, Fusion Zone (FZ), Heat Affected Zone (HAZ), and Base Metal (BM) that exhibits nonhomogeneous microstructures and properties therefore different mechanical strength in each zone as well as strength mismatch between the zones that form strain concentration at the weakest side. Additional to the heterogeneity, geometrical factors reduce the load-bearing capacity of the joints for examples, indentation, the micro-voids in the FZ and crack-like tip of the gap into the FZ [2]. Chabok et al. [3] separated the HAZ region into the Coarse grain HAZ (CGHAZ), the Fine grain HAZ (FGHAZ), and the Inter Critical HAZ (ICHAZ) and experimentally extracted mechanical and fracture properties of each region for DP1000 steel.

When evaluating a welded joint’s performance, the complexity of dealing with these factors usually leads to relying on physical welding trials to set the process parameters and examine the performance. An alternative is the digital twin of the process that captures the physics of welding for simulating the performance of joint once loaded [4]. However, constructing a proper digital twin of automotive components, which include multiple welds, can be labour intensive and could take long CPU time to analyze. This disadvantage is mainly due to the local variation of microstructure and properties in the weld, and HAZ that needs fine mesh and various materials definition when building the model. Majority of modellers take the shortest path toward the simplification of the problem and ignore any local change around the weld and limit the analysis to a simple mechanical definition with spot weld as a mechanical tie between to surfaces. These models are efficient for load carrying analysis at the component level where the objective is not an investigation of failures such as fatigue or crash. In other words, failure is a local phenomenon and cannot be adequately investigated without adding local features to the model.

Ford Motors [5] improved the prediction by introducing spring elements where the separation of the spot weld was defined by levels of peak force, displacement and energy. Another simple solution is a model that represents spot weld as beams [6] where the beams connect shell elements. The diameter of the beams was formulated by dividing the area of the cross-section of the representative spot weld with the number of beams. If the correlation between experiment and model was built correctly, these approaches could investigate a general failure of spot welds (i.e. fail/no fail binary decision) under loading conditions.

The mechanical properties of the weld and surrounding subzones are not easy to obtain due to the small size of the zones. Some techniques can experimentally simulate the thermal profile of weld and form similar microstructure but uniform and at a larger size for measuring the properties. Yet, once these properties are available, defining the zones with these properties are time-consuming at the component level with many spot welds. Therefore a typical approach is to model a single-spot-weld [7] and map or replace the other welds with this single-spot-weld. This characteristic spot weld can be one of all welds in the component. In this paper, we form the digital twin of a car component subjected to crash where we utilized all weld zones in the analysis.

2. Automotive Component

Fig. 1 shows the spot-welded automotive component used for crash analysis in this paper. The component consists of an omega-shaped and a plate, made of DP1000 dual-phase high-strength steel profiles, showing a total length of 300 mm. Both parts are bonded together at the flanges of the omega section, through spot welds showing 8mm diameter, and equal spacing between them, 30 mm.

3. Digital Spot Welding

A full 3D model of each weld was created using in-house subroutines. The subroutine uses the fying surfaces for fusion line defined by the user and assigns a heat flux by Joule’s law which in its purest form can be expressed by the Eq. 1.

$$H = RI^2t \qquad \text{Eq. 1}$$

where is the weld heat input in joules, I is the current in amperes, R is the resistance in ohms and t is the time in seconds. A series of cool down steps were added after the welding was performed to model the returning thermal profile to ambient temperature.

The initial temperature was 21 °C. A convection boundary condition generated a boundary flux on all external surfaces. The total temperature-dependent convection coefficient is computed from Eq. 1 where T is the temperature in °C [8].

$$h_c = 5 + 0.05\,(T - 20) + 6 \times 10^{-7}\,(T - 20)^3$$

Eq.2

Below are the properties are taken from [9] and [10] for this welding analysis:

- Temperature-dependent Thermal Conductivity
- Temperature-dependent Thermal Expansion
- Temperature-dependent Heat Capacity
- Temperature-dependent Module of Elasticity
- Temperature-dependent Yield Stress
- Temperature-dependent Density
- Poisson's ratio

Fig. 2 shows the result of the simulation, including the formation and evolution of weld nugget on the automotive spot-welded component of interest in this paper.

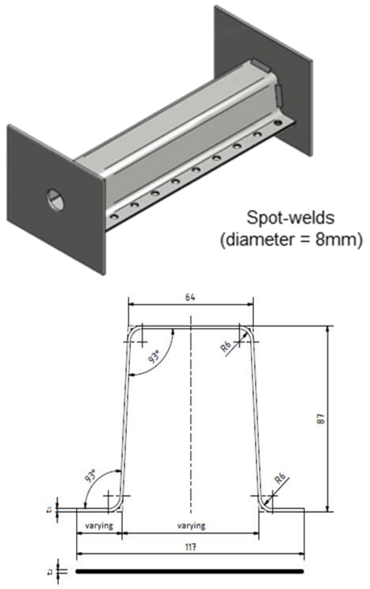

Fig. 1 **Automotive component used for analysis in this paper.**

4. Digitization of Microstructure Evolution

During the heating cycle, the equilibrium transformation temperature starts forming Austenite at A1 (≈800 °C) and becomes fully Austenitic above A3 (≈900 °C). During welding, the available time between A1 and A3 is short for equilibrium transformation and therefore the Austenization finishes above the A3 by massive recrystallization due to the superheating rather than diffusion. Higher temperature activates the Austenite grain growth by merging and migrating grain boundaries; however, the existence of Carbide and Nitrides precipitate blockades this migration until a critical temperature Ts (≈1100 °C) when the precipitates dissolve into the Austenite matrix and allow the Austenite grain growth. During Cool down, the grain growth continues below A3 when the Austenite decomposition starts mostly by supercooling nucleation on the boundary of large Austenite, the formation of Bainite below, Bs (≈500 °C) and Martensite below Ms (≈400 °C).

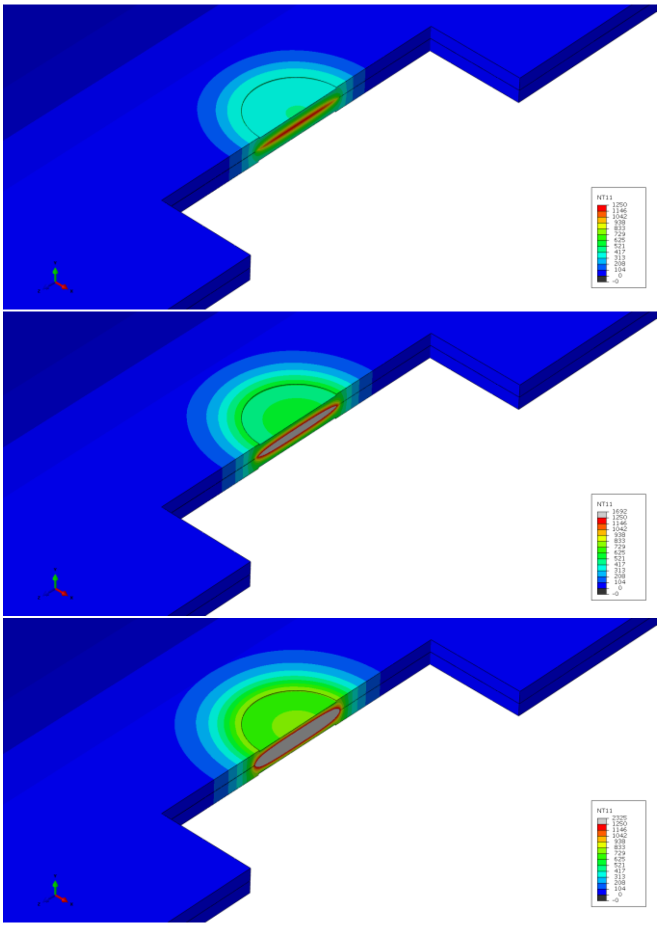

Fig. 2 **Formation and evolution of weld nugget (gray colour) on the automotive spot-welded component of interest.**

Two parameters of a welding thermal profile can define the microstructure of HAZ, namely, the peak temperature and cooling rate [11]. The peak temperature primarily depends on the distance to the fusion line and the cooling rate depends on the overall heat sink in the joint. Using our welding simulation tool for spot welding, we showed that the heat sink is approximately constant for every peak temperature on a given joint and spot welding process. Therefore, we used the welding simulation for forming thermal profiles associated with every location of HAZ and pick the typical cooling rate at every pick temperature without losing a substantial precision of predicting the final microstructure.

This assumption simplifies the microstructure models as a function of peak temperature such that a relationship was created between the final microstructure and the trajectory of the peak temperature for the critical transformation temperature. Fig. 3 shows that simulation result for ICHAZ, FGHAZ, CGHAZ, FZ regions that formed during our welding process. Table 1 summarizes the mechanical properties of each region used in the analysis [12].

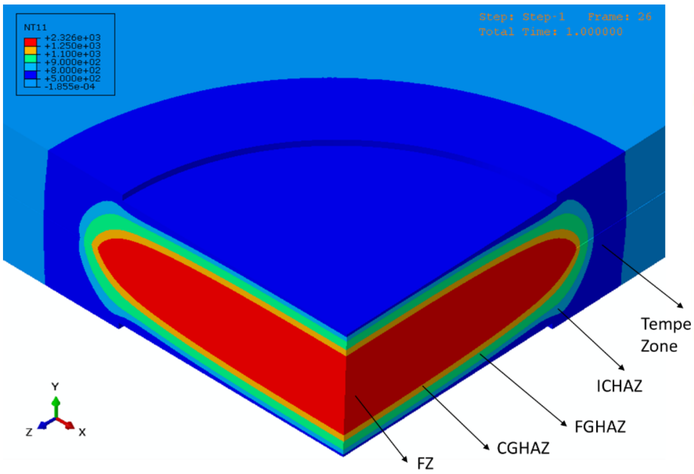

Fig. 3 Simulation result that defines each region of HAZ.

Microstructure Region	Elasticity (GPa)	Hardness (HV)	Yield (MPa)	UTS (MPa)	Strain at UTS
FZ	234	510	1175	1350	0.07
CGHAZ	226	450	1514	1740	0.08
FGHAZ	239	420	1940	2000	0.1
ICHAZ	228	390	1159	1212	0.06
Tempered	219	280	662	1000	0.05
Unaffected	219	290	662	1000	0.05

Tab. 2 Mechanical properties of each region used in the analysis.

5. Experimental Crash Testing Set-up.

An axial impact test of a steel beam subjected to different velocities is used in this work as a validation method for the presented spot weld modeling methodology. A schematic view of the test configuration can be found in Fig 4. Samples are tested under different speeds ranging from 10 to 40 km/h, driven by a mass of 283 kg. The objective of the test is to study the correlation of the experimental force versus displacement curves with those obtained by simulation, using different approaches toward spot weld characterization and modeling.

6. Digital Crash Testing Set-up.

A finite element model representing the test configuration is created using LS-Dyna. The DP1000 steel is modeled using shell elements with the corresponding plate thickness. It is defined using the MAT24 material model and enriched through the methodology. It is essential to mention that the permanent effects produced in the material due to a cold forming procedure on the omega-shaped beam are introduced in the model.

Fig. 4 Axial impact test set-up on a DP1000 steel beam used as a validation method.

For this cold forming effect, an initial plastic strain is introduced in the regions defined by the profile edges, obtained from the simulation of the manufacturing process. The definition of these regions with respect to the rest of the beam profile can be observed in Fig. 5. Spot welds are modeled using a combination of solid elements representing the nugget, and a crown of shell elements representing the HAZ. Material characterization of these elements has been carried out using IDIADA HAZ methodology, which is explained further on. Weld seams joining the beam ends to the vertical faces of the testing device are modeled by shell elements, defined by the same material as the one used in spot weld nugget.

Four impact tests using different velocities are performed, comparing in every case, the performance of the two proposed HAZ discretization scales.

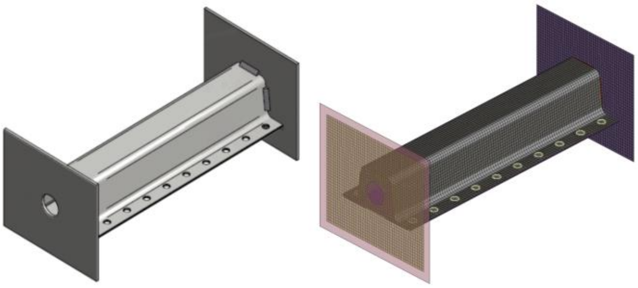

Fig. 5 Schematic representation (left) and FEM model (right) of the axial impact sample.

7. Digitization of Spot-Welds for Crash Simulations

Each of the microstructure regions (i.e. FZ, CGHAZ, FGHAZ, ICHAZ) shows different mechanical properties; therefore, spot weld modeling should represent such properties accurately without conditioning the original mesh size and time step.

Spot weld modeling of components for automotive crash simulations is performed using LS-Dyna software. This modeling is done using two different approaches – namely, mesoscale and automotive scale – depending on the detail in the definition of the HAZ. In both scales, an aggregation of solid elements is used for the representation of the spot weld nugget. This part is attached to the surrounding base material through a crown formed by shell elements representing the different parts of the HAZ, as can be seen in Fig. 6. The generation of these elements is done over the contact surfaces of the component, with the help of the connection manager tool of ANSA pre-processor.

Both in the case of mesoscale and automotive scale models, spot weld nugget is represented by four hexahedra, whose bases together form an octagon in which the distance between opposite vertices is equivalent to the nominal diameter of the spot weld. The solids from the nugget are defined by a thickness equal to the separation between the middle planes of the sheets since these are modeled by shell elements. This fact must be taken into account when defining the elasticity of the nugget. In the mesoscale model, the width of the shell crowns that define both zones of thermal affectation is directly taken from the results of the performed microanalysis, explained above. ICHAZ has been neglected in the numerical models, due to its relatively small size and insignificant influence in the obtained results. The whole spot weld, consisting of two sub-zones of thermal affectation (FCHAZ, CGHAZ) plus the nugget, is defined using the LS-Dyna material model MAT24 MAT_PIECEWISE_LINEAR_PLASTICITY, which is also used to model the physical behaviour of the unaffected base material.

A comparison of the geometrical definition of a generic spot weld on the mesoscale and automotive scale is shown in Fig. 6. As can be seen, the most noticeable difference between the two exposed geometries lies in the discretization of the HAZ. One of the main drawbacks that the analyst faces at the time of setting up a numerical model is the definition of an appropriate time step for the simulation, limited by the Courant stability criterion. In explicit simulations, mass scaling of individual elements is a common practice, carried out to increase the time step sufficiently. The added mass is often assumable when it is relatively small and distributed over the entire geometry, or large but concentrated in non-critical areas. Also, it can be dismissed when it takes place in quasi-static simulations in which kinetic energy is minimal compared to internal energy. However, in many cases, mass scaling can negatively affect the physical behaviour of the model. It is, therefore, a task of the analyst to evaluate the effects that this measure can have on the simulation results.

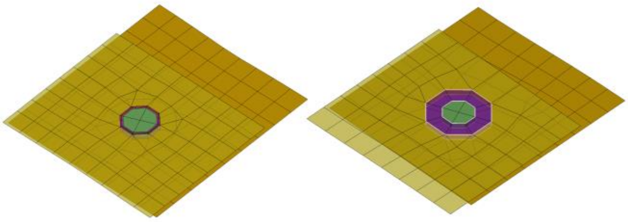

Fig. 6 Detail view of the FEM definition of a spot weld using the two proposed scales: mesoscale (left) using element size from microstructural analysis of spot welding process, and automotive scale (right) using an element size according to the discretization of surrounding base material.

In this sense, the localized mass increase in the tested components was checked during this work. The mesoscale model serves as a subsequent step after the micro-definition of spot welds described in previous sections. This approach is used to characterize the different zones of the HAZ, but it is not useful in complex cases such as Full Vehicle crash simulations. In these cases, it is fundamental to minimize the addition of mass to the whole model, although spot welds are generally dispersed throughout a vehicle body-in-white. The definition of a macroscale model for spot welds is then mandatory. It gathers the properties of the different zones of the HAZ in a single crown of shell elements of similar size to those that define the base material. This approach allows keeping a minimum time step of 0.5×10^{-4} ms without an excessive introduction of added mass.

The starting point of the characterization process of the spot weld regions is the material card of the unaffected steel, applying a series of transformations based on the results arising from the microstructural analysis. LS-Dyna material model MAT24 represents an elasto-plastic material in which the plasticity is dependent on the strain-rate. A subsequent enrichment allows a detailed description of the physical behaviour of the steel. As the first step, the characterization of the plastic regime, based on an analytical approach, is capable of capturing the post-necking behaviour during the realization of tensile tests on any steel sample. On the other hand, the damage initiation envelope is obtained through analytical methods enriched by detailed simulations of such tensile test. Finally, the evolution of failure is defined to obtain mesh-independent behaviour.

IDIADA HAZ plasticity prediction model has obtained plasticity curves corresponding to each zone of the spot weld. This model is based in the Ultimate Tensile Strength (UTS) values provided by the microstructural analysis, which allows predicting the modified properties from the Base Material.

Additionally, the damage initialization and the failure envelopes at each zone are estimated by IDIADA HAZ damage prediction model. This model generates an estimated analytical damage initialization and the failure envelopes based on Energy dissipation criteria.

In the automotive scale, mechanical properties are gathered into a single crown by applying the mechanical properties of the most fragile part of the spot weld to the whole HAZ.

8. Crash Simulation Results

A comparison of simulation results with experimental data is shown in Fig. 7. It can be observed that the elastic regime of the curve is adequately captured in faster velocity scenarios, whereas a certain lack of accuracy arises in the case of impacts at lower velocities. A similar behaviour observed at the peak force. For instance, simulation results for testing at 23.4 km/h accomplish a high level of correlation of the first part of the curve either using the mesoscale or the automotive scale mesh. Maximum force value of 339 kN is comparable to values of 341 kN with the mesoscale and 333 kN with the automotive scale approach. At lower velocities, Unless using mesoscale, the stiffness and peak force are smaller than expected from experimental results. For instance, at 14.1 km/h the experimental maximum force is 358 kN, while simulations reach values of 273 kN and 270 kN for the mesoscale and the automotive scale, respectively. Simulations also show a lack of precision in the first energy release as the beam collapses. Since the choice of one discretization scale or another does not have any effect in that sense, it is feasible to consider a direct relation between the energy released by the model and the deformation of the weld seams at each beam end. This relationship is confirmed by the fact that a finer discretization of the mesh does not lead to an improvement in the quality of the results in this area. Thus, a more accurate definition of weld seams elements can lead to a better correlation of this part of the curve.

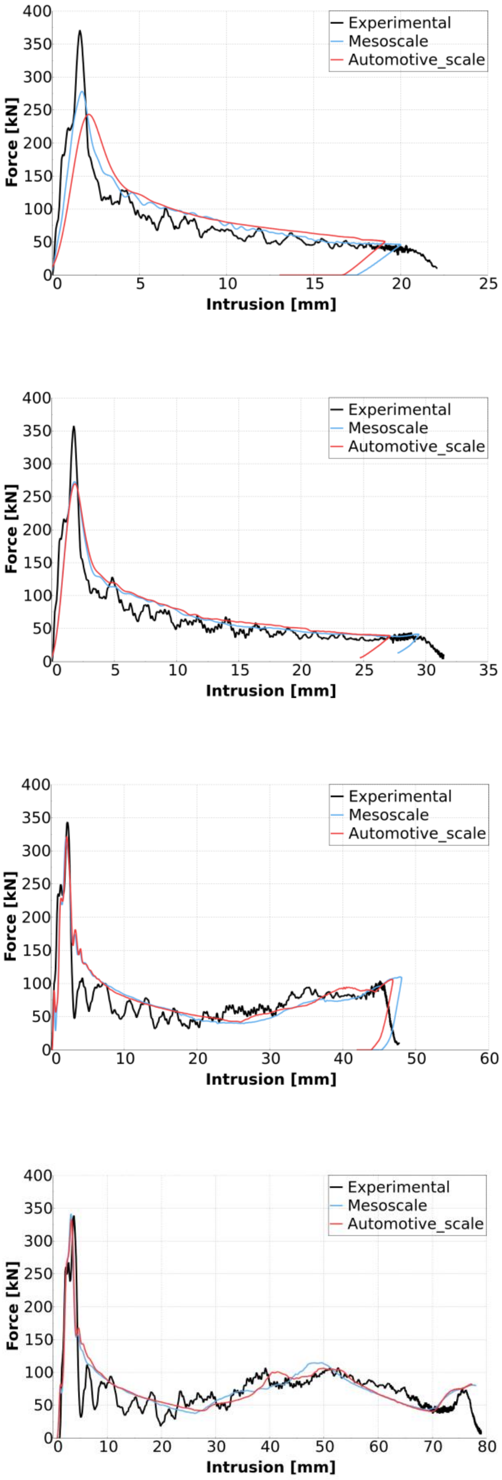

Fig. 7 Comparison of experimental and simulation results under different velocities (i.e. 12.9, 14.1, 18.6 and 23.4km/h from top to bottom), model using two discretization levels in the HAZ.

Fundamental phenomena to be taken into account in crash simulations such as propagation of failure, intrusion, beam folding and deterioration of spot welds are properly captured by the proposed numerical models, both at meso and automotive scales. The accuracy is even higher in the case of lower velocities.

Also, as happens in reality, a different number of folds appears depending on the velocity at which the sample impacts with the rigid wall. The review of the deformed geometry shows, compared to the experimental results, an excellent accuracy of the model predicting complex failure phenomena at spot welds such as unbuttoning, base material tearing or spot weld cracking, depicted at Fig. 8 and Fig. 9. Finally, it is essential to highlight the fact that certain aspects of the simulation, such as the peak values or area of collapse, show high sensitivity to minimum changes performed in the geometry of the model, such as the distribution of the spot welds or weld seams length or thickness.

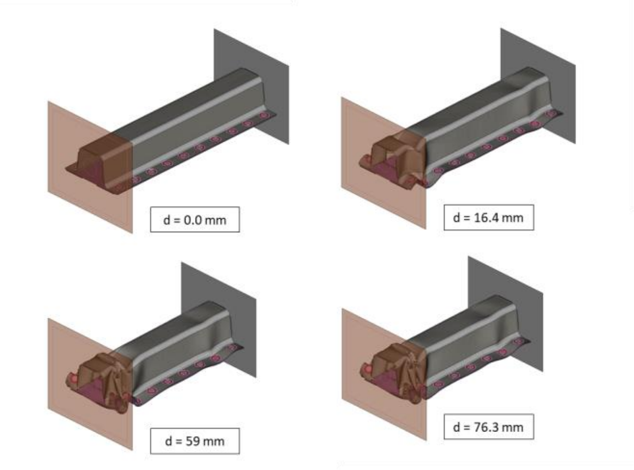

Fig. 8 **General view of an axial impact test, showing its deformed geometry in different stages of the simulation,**

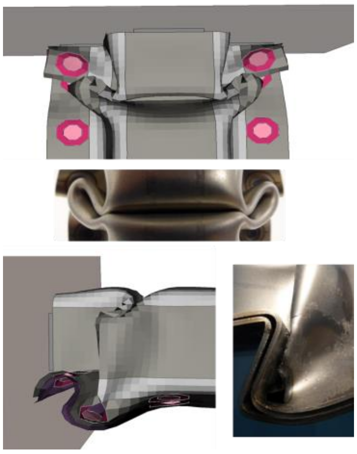

Fig. 9 **Details of the different failure modes on spot welds that arise from the simulation at d = 38 mm of an axial impact test.**

9. Microstructure Dependency vs. Mechanical Tie.

This section compares the results obtained using the modeling approach described in this paper and the classical approach where the spot weld nugget is represented using an aggregation of solid elements, and the HAZ properties are not taken into account. The size of the nugget in the classic approach is identical to that used in the proposed methodology. The material used to define the nugget, in this case, is the LS-Dyna MAT100 MAT_SPOTWELD_DAMAGE-FAILURE. The bond between these solids and the beam flanges is made through tied-type contacts, as can be observed in Fig. 10.

Definition of the base material, weld seams as well as boundary conditions is identical to that used in the precious models presented. A comparison of the results is shown in Fig. 11. It can be seen that the section of the curves corresponding to the initial deformation and collapse of the beam are similar because, as mentioned, modeling of the base material and weld seams is equivalent in both cases. The most noticeable difference between the compared approaches takes place in the damaged regime of the curve. When comparing the damage propagation across the component, it is observed that in general, the curves obtained by classical approach overestimate the force supported, and further away from the experimental values. As a consequence, classical modeling predicts lower intrusion values at all velocities, which is, as mentioned above, a key factor to be taken into account when performing automotive crash simulations.

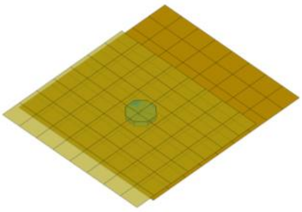

Fig. 10 Detail view of a spot weld using a traditional approach.

Compared to the traditional way of modeling spot welds – using beams or solid elements attached to the base material through tied contacts – the approach presented in this work allows a more precise definition of the different material properties from each of the entities that form the spot weld. Thus, more accurate simulations compared to reality are obtained. In this regard, the deformed geometry can represent the complex failure modes that are susceptible to appear during crash testing of components joined with spot welds, including phenomena like nugget cracking, unbuttoning or base material tearing.

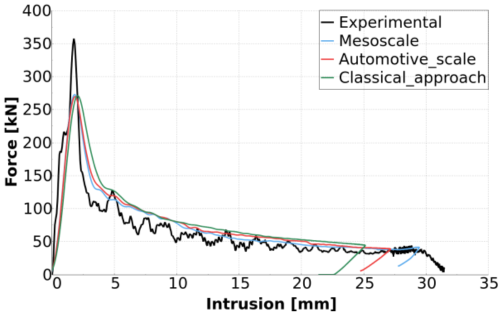

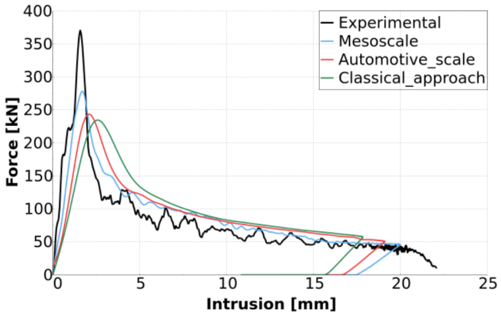

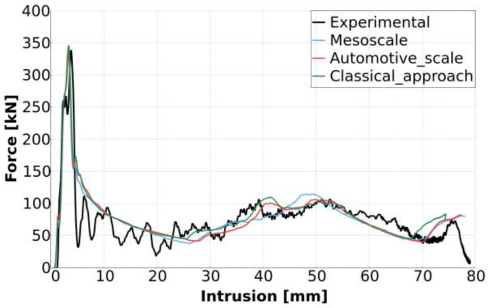

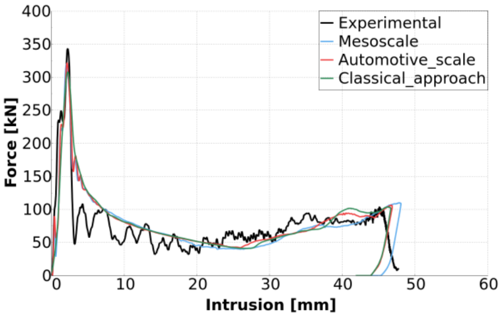

Fig. 11 Comparison of experimental and simulation results of the axial impact test performed on a DP1000 steel beam under different velocities, modeled using the proposed HAZ definition from microstructural analysis and a traditional approach.

10. Conclusion.

Crash performance evaluation of the welded joint relies on the level of welding details considered. Defining the weld as a mechanical tie between two sheet metals is the fastest and most straightforward approach but remains blind to any local variation of microstructure and properties in the weld, and HAZ. These models can give insight toward the load carrying capacity of welded components; however, failure analysis of crash cannot be investigated adequately without adding local weld properties to the model. On the other hand, constructing a full digital twin of automotive components, which include multiple welds, can be less practically feasible because of fine mesh and various materials definition in welds and HAZs. With the current power of computation and automation in meshing, evidence recommends modeling a single-spot-weld that can characterize many welds then use it for other welds. The thicknesses, material combination, and heat sink around the weld can be useful criteria for defining the characteristic weld. While this approach saves time in the evaluation, it builds weld details in the evaluation for capturing local performances, including failure and fractures.

Acknowledgements

The authors sincerely acknowledge the support by the team of Simulation at Applus IDIADA (Santa Oliva, Spain) with special thanks to Eduardo Martin, Alfredo Alameda, Sudip Chandratre, Monica Cartanya, and Ines Lama for their expertise and assistance throughout all aspects of this work and for their help in conducting high quality crash simulations.

References

[1] V. P. Dipak and A. S. Ganesh, "A Review on Effect of Spot Weld Parameters on Spot Weld Strength Weld Strength," International Journal of Engineering Development and Research, vol. 3, no. 1, 2014.

[2] M. Pouranvari and P. Marashi, "Critical review of automotive steels spot welding: process, structure and properties," Science and Technology of Welding and Joining, vol. 18, no. 5, pp. 361-403, 2013.

[3] A. Chabok, E. GaliGalinmoghaddam, J. De Hosson and Y. T. Pei, "Micromechanical evaluation of DP1000-GI dual-phase high-strength steel resistance spot weld," J Mater Sci, vol. 54, p. 1703–1715, 2019.

[4] O. Andersson, D. Semere, A. Melander, M. Arvidsson and B. Lindberg, "Digitalization of Process Planning of Spot Welding in Body-in-white," Procedia CIRP, vol. 50, pp. 618-623, 2016.

[5] O. Faruque, N. Saha, K. Mallela, T. Tyan and C. Madasamy, "Modeling of Spot Weld under Impact Loading and Its Effect on Crash Simulation," in SAE International published, 2006.

[6] A. S. AJALAKSHMI and T. SHAFIQ, Modeling of Spot Weld with Failure, Gothenburg, Sweden: Master's thesis in Automotive Engineering, Department of Applied Mechanics, CHALMERS UNIVERSITY OF TECHNOLOGY, 2017.

[7] H.-Y. Hwang and N. Q. Nghiem, "Spot Weld Property Testing and Simulation Modeling with Failure Criteria," Applied Mechanics and Materials, Vols. 284-287, pp. 198-203, 2013.

[8] J. Goldak and M. Akhlaghi, Computational Welding Mechanics, ISBN-10: 0-387-23287-7: Springer, 2005.

[9] N. J. Den and Ujil, "Thermal and Electrical Resistance in Resistance Spot Welding," in 17th International Conference Computer Technology in Welding and Manufacturing, Cambridge, United Kingdom, 2008.

[10] "Characteristics of multi-pass narrow-gap laser welding of D406A ultra-high strength steel," J of Materials Processing Technology, vol. 270, pp. 168-181, 2019.

[11] J. C. Ion, Modeling the Microstructural Changes in Steels due to Fusion Welding, PhD Thesis: Lulea University of Technology, 1984.

[12] A. Chabok, E. Galinmoghadam, J. T. M. De Hosson and Y. T. Pei, "Micromechanical evaluation of DP1000-GI dual-phase high-strength steel resistance spot weld," J Mater Science, vol. 54, pp. 1703-1715, 2019.